1   **Developmental Genome-Wide DNA Methylation Asymmetry Between**

2   **Mouse Placenta and Embryo**

3

4   Legault LM[1,2], Doiron K[1], Lemieux A[1,2], Caron M[1,3], Chan D[3], Lopes FL[4], Bourque G[5,6,7],

5   Sinnett D[1,8], McGraw S[1,2,9, #].

6

7   [1]Research Center of the CHU Sainte-Justine, Montreal, Canada.

8   [2]Department of Biochemistry and Molecular Medicine, Université de Montréal, Montreal,

9   Canada.

10   [3]Research Institute of the McGill University Health Centre, Montreal, Quebec, Canada

11   [4]São Paulo State University (Unesp), School of Veterinary Medicine, Aracatuba, Brazil

12   [5]Department of Human Genetics, McGill University, Montreal, Quebec, Canada

13   [6]McGill University and Genome Quebec Innovation Centre, Montreal, Quebec, Canada

14   [7]Canadian Center for Computational Genomics, Montreal, Quebec, Canada

15   [8]Department of Pediatrics, Université de Montréal, Montreal, Canada.

16   [9]Department of Obstetrics and Gynecology, Université de Montréal, Montreal, Canada.

17

18   [#]Corresponding author: serge.mcgraw@umontreal.ca

19

20

21   **Running title:** Embryonic & Placental DNAme Asymmetry

22

23   **Summary statement:** The kinetics of asymmetric DNA methylation acquisition of embryo-

24   placenta differentially methylated regions is not a stepwise process occurring in embryonic and

25   extraembryonic lineages, but a prompt progression in the early post-implanted conceptus.

26

1

ABSTRACT

In early embryos, DNA methylation is remodelled to initiate the developmental program but for mostly unknown reasons, methylation marks are acquired unequally between embryonic and placental cells. To better understand this, we generated high-resolution DNA methylation maps of mouse mid-gestation (E10.5) embryo and placenta. We uncovered specific subtypes of differentially methylated regions (DMRs) that contribute directly to the developmental asymmetry existing between mid-gestation embryonic and placental DNA methylation patterns. We show that the asymmetry occurs rapidly during the acquisition of marks in the post-implanted conceptus (E3.5-E6.5), and that these patterns are long-lasting across subtypes of DMRs throughout prenatal development and in somatic tissues. We reveal that at the peri-implantation stages, the *de novo* methyltransferase activity of DNMT3B is the main driver of methylation marks on asymmetric DMRs, and that DNMT3B can largely compensate for lack of DNMT3A in the epiblast and extraembryonic ectoderm, whereas DNMT3A can only partially palliate in the absence of DNMT3B. However, as development progresses and as DNMT3A becomes the principal *de novo* methyltransferase, the compensatory DNA methylation mechanism of DNMT3B on DMRs becomes less effective.

INTRODUCTION

Throughout the eutherian mammalian gestation, the placenta plays an essential role in mediating maternal–embryonic exchanges of gas, nutrients and waste, and also provides the developing embryo with a protective layer against adverse environmental exposures and the maternal immune system (Rossant and Cross, 2001). These unique placental functions are orchestrated by several distinct trophoblast cell subtypes organized in separate layers (Cross, 2000). The initial steps of lineage specialization of both placental and embryonic cells occur promptly following fertilization during the first few embryonic cleavages as DNA methylation marks are being reprogrammed (Morgan et al., 2005).

DNA methylation is an epigenetic mechanism that is critical in the determination of lineage-specific differentiation and development, and is mainly recognized for its involvement in processes such as transcriptional repression, genomic imprinting and X-inactivation (Bestor, 2000). DNA methylation marks are mediated by the action of DNA methyltransferases (DNMTs). Establishment of new or *de novo* DNA methylation patterns required for cell lineage determination during development is mediated by DNMT3A and DNMT3B, with cofactor DNMT3L, (Okano et al., 1999, Li, 2002), whereas DNMT1 maintains heritable DNA methylation patterns during cellular divisions (Leonhardt et al., 1992, Lei et al., 1996). These enzymes are critical, as deletion of *Dnmt3b* or *Dnmt1* is embryonic lethal, while *Dnmt3a*-deficient offspring die shortly after birth (Li et al., 1992, Okano et al., 1999). During gametogenesis, the acquisition of genome-wide and allele-specific methylation patterns (i.e. genomic imprinting) in both oocytes and sperm is essentially due to the activity of DNMT3A (Kaneda et al., 2004, Kato et al., 2007). Following fertilization, a reprogramming wave removes most methylation signatures across the genome, except for imprinted regions, some types of repeat sequences, as well as imprinted-like sequences, to trigger the developmental program (Hirasawa et al., 2008, Howell et al., 2001, McGraw et al., 2015). Then, during the peri-implantation process, DNA methylation profiles are re-acquired in a sex-, cell- and tissue-specific manner across most parts of the genome by the combined action of DNMT3A and DNMT3B. In the early stages of the *de novo* methylation wave (E4.5-E7.5), the expression of *Dnmt3b* is more robust than *Dnmt3a* in the epiblast and embryonic-derived cells (Watanabe et al., 2002, Auclair et al., 2014, Smith et al., 2017), with the relative expression of *Dnmt3b* and *Dnmt3a* being considerably reduced in the extraembryonic ectoderm (ExE) and trophoblast

3

75   lineages (Smith et al., 2017, Senner et al., 2012). This discrepancy in *Dnmt3a* and *Dnmt3b*
76   expression levels coincides with the initiation of divergent DNA methylation acquisition
77   between the trophoblast and the inner cell mass of the blastocyst (Monk, 1987, Nakanishi et al.,
78   2012, Oda et al., 2013, Santos et al., 2002, Fulka et al., 2004, Guo et al., 2014, Smith et al.,
79   2014), a difference that becomes extremely apparent by E6.5, as the epiblast has acquired most
80   of its global DNA methylation compared to the lower-methylation state of the ExE (Auclair et
81   al., 2014, Smith et al., 2017). This divergence is a common feature across mammalian placenta,
82   as a heterogeneous and lower-methylation state compared to somatic tissues and other cell types
83   is constantly observed (Smith et al., 2017, Decato et al., 2017, Schroeder et al., 2013, Chatterjee
84   et al., 2016).

85   Although the functional role of reduced methylation levels observed across the placental
86   genome is still not fully understood, studies suggest that it may activate transposable elements
87   that are typically silenced in other tissues (Chuong, 2013). DNA methylation plays an important
88   role in suppressing retrotransposons in mammalian cells, for which the activity has been
89   associated with genomic instability and disease development (Church et al., 2009, Slotkin and
90   Martienssen, 2007). Following the *de novo* methylation wave, in embryonic-derived cells from
91   the inner cell mass, transposable elements acquire higher levels of DNA methylation causing
92   transcriptional silencing, whereas in the trophectoderm-derived cells that will form the placenta,
93   these transposable elements are maintained in a relaxed methylation state and preferentially
94   expressed (Price et al., 2012, Okahara et al., 2004, Warren et al., 2015). The low-methylation
95   levels on these elements contributed to the evolution and diversification of the placenta function
96   through the regulation of gene expression by providing placenta-specific enhancers, cryptic
97   promoters and other cis-regulatory elements (Haig, 2012, Mi et al., 2000, Cohen et al., 2011, Xie
98   et al., 2013, Macaulay et al., 2011, Emera and Wagner, 2012).

99   Despite the evident distinction between embryonic and placental DNA methylation
100   levels, it remains unclear how, when and where methylation levels are acquired unequally across
101   these genomes. To better understand the developmental dynamics of epigenetic asymmetry that
102   exists between embryo and placenta, we first generated high-resolution maps of DNA
103   methylation marks using Reduced Representation Bisulfite Sequencing (RRBS) at mid-gestation,
104   when the mouse placenta is first considered mature (E10.5), to identify embryo-placenta
105   differentially methylated regions (DMRs). Then, using publicly available DNA methylation data

106   sets and computational analyses, we defined how various categories of DMRs are established in

107   early stages and maintained throughout development. In addition, we outlined the contribution of

108   *Dnmt3a* and *Dnmt3b* in the acquisition and maintenance of embryonic and extraembryonic

109   specific DMR patterns.

110

111   **METHODS**

112   *Animals and Sample Collection*

113   Female C57BL/6 (8-10 week-old) were purchased from Harlan Sprague-Dawley

114   Laboratories (Indianapolis, IN) and were mated with male C57BL/6 (4 months of age).

115   Following natural mating, embryos and placental tissues were collected at E10.5 (presence of

116   vaginal plug at E0.5). Samples were frozen immediately in liquid nitrogen and stored at -80 °C

117   until analyzed.

118

119   *DNA Methylation Analyses*

120   RRBS libraries were generated as published protocols (Boyle et al., 2012, Gu et al., 2011)

121   with our specifications (Magnus et al., 2014, McGraw et al., 2015, Legault et al., 2019). 500 ng

122   of extracted DNA (Qiagen) from placenta (male n=2, female n=2) and embryo (male n=2,

123   female n=2) samples was *MspI* digested, adaptor ligated and PCR amplified (multiplex).

124   Multiplexed samples were pooled and 100 bp paired-end sequenced (HiSeq-2000, Illumina). The

125   data analyses were done according to the pipeline established at the McGill Epigenomics

126   Mapping and Data Coordinating Centers (Magnus et al., 2014, McGraw et al., 2015) that include

127   BSMAP and methylKit. Specific parameters were chosen including 100 bp step-wise tiling

128   windows, containing a minimum of 2 CpGs per tile and a minimum $15\times$ CpG coverage of each

129   tile per sample. The methylation level of a 100-bp tile was the result of all CpG C/T read counts

130   within the tile after coverage normalization between samples, and the methylation level reported

131   for a sample on autosomal chromosomes was the average methylation level across replicates.

132   Significant DNA methylation changes were designated as $\pm\geq20\%$ average differences between

133   groups of replicates and a q-value < 0.01 using the logistic regression function of methylKit

134   (Akalin et al., 2012). Direct comparisons between DNA methylation averages were done using

135   Wilcoxon-Mann-Whitney test in R. Gene ontology (GO) terms and pathway analyses for

5

136 RefSeqs associated to promoter-TSS were conducted using Metascape gene annotation and

137 analysis resource (Zhou et al., 2019).

138

139 *Sequencing Data*

140   Publicly available DNA methylation data sets (Auclair et al., 2014, Decato et al., 2017,

141 Smith et al., 2014, Smith et al., 2017, Whidden et al., 2016, Hon et al., 2013) were analyzed

142 using a custom script to intersect single CpG site methylation calls from these data sets within

143 defined 100bp tiles associated to the embryo-placenta DMRs categories

144

145 **RESULTS**

146 *Increased Fluctuation in Genome-Wide DNA Methylation Levels in Placental Cells*

147   To identify the overall epigenetic asymmetry that exists between placental and embryonic

148 genomes during mouse *in utero* development, we first established genome-wide DNA

149 methylation profiles using RRBS (McGraw et al., 2015, Magnus et al., 2014, Legault et al.,

150 2019) of embryos and their corresponding placentas at mid-gestation (E10.5), the developmental

151 stage at which the mouse placenta is considered mature (Cross et al., 1994). Using this approach,

152 we quantified the DNA methylation profiles of ~1.8 million CpG sites in each sample (embryo

153 n=4, placenta n=4). We found that the accumulation of CpG methylation was very distinct

154 between the placenta and the embryo. In the placenta, we detected a greater proportion of CpGs

155 in the 0-50% methylation range and a lower proportion of CpGs in the 80-100% methylation

156 range (Figure 1A). Although we observed that a large proportion of CpGs within the examined

157 regions had no methylation marks in both the embryo and the placenta, interestingly, most CpGs

158 with partial methylation (20-50%) in placenta showed high methylation levels (>80%) in

159 embryos (Figure 1B). The divergence in global DNA methylation profiles conferred a high

160 degree of clustering between both tissue types (Figure S1). These results are consistent with

161 previous studies indicating lower levels of overall DNA methylation in extraembryonic tissues

162 (Price et al., 2012, Schroeder et al., 2013, Smith et al., 2017), reviewed in (Robinson and Price,

163 2015).

164   To further investigate the dynamics of DNA methylation between placental and

165 embryonic genomes and enable direct comparison of precise regions, we segmented the genome

166 of autosomal chromosomes into 100bp non-overlapping genomic windows (*tiles*; see methods

6

167   section). After removal of sex chromosomes, we identified 245 048 unique sequenced tiles

168   (referred to as All-tiles) containing 896 820 common CpGs between all placenta and embryo

169   samples and with a minimum of 15x sequencing depth. We observed a strong reduction in the

170   fraction of highly methylated tiles (80-100%) in the placenta compared to the embryo (Figure

171   1C), which correlated with a sharp increase in the number of placenta tiles in the 0-20%, 20-40%

172   and 40-60% methylation range. Globally, we found that the average DNA methylation level

173   across all placental tiles was significantly lower compared to all embryo tiles (27% vs 45%,

174   p<0.0001) (Figure 1C). This overall epigenetic disparity in embryo and placenta DNA

175   methylation levels was especially noticeable when we mapped the methylation mean of All-tiles

176   with respect to regions surrounding the transcription start sites (TSS) (Figure 1D). When we

177   focused on a specific chromosome section (e.g., chr 7, 35Mb) (Figure 1E), we observed that

178   genomic segments with high DNA methylation levels in embryos were predominantly

179   hypomethylated in placenta. We also observed that gene or CpG island (CGI) poor regions had

180   consistently high methylation levels in embryos and lower methylation levels in the placenta.

181   Together, these results indicate that the mid-gestation placenta has very distinctive global DNA

182   methylation profiles compared to the embryo, and that this lower level of global DNA

183   methylation (i.e., DNA hypomethylation) across the placental genome is due to a significant

184   lower number of highly methylated (≥80%) genomic regions. We can also conclude that despite

185   the cellular heterogeneity in E10.5 placental and embryonic tissues, the vast majority of the

186   conceptus possesses specific genomic regions with either low (0-20%) or high (80-100%) levels

187   of methylation. However, the placenta genome presents an increased number of regions having a

188   broader distribution of DNA methylation (20-80%), revealing a greater diversity in methylation

189   levels across placental cell types compared to embryonic cell types.

190

191   *Embryonic and Placental DNA Methylation Divergences Across Genomic Features*

192   To explain the developmentally divergent methylated states between the mouse embryo

193   and the placenta, we next sought to precisely determine the genomic features revealing DNA

194   methylation differences. We defined differentially methylated regions (DMRs) as 100bp

195   genomic segments showing a significant difference of methylation levels between embryonic

196   and placental samples with an absolute mean methylation difference of 20% or higher (McGraw

197   et al., 2015, Shaffer et al., 2015, Piche et al., 2019). Using these conditions, we screened the 245

198   048 unique tiles common between all samples and identified 110 240 DMRs (~45% of All-tiles;

199   Supplementary Table 1) with tissue- and/or developmental-specific DNA methylation variations

200   between the embryo and the placenta (Figure2A; random subset of 20,000 DMRs shown).

201   Consistent with our findings (Figure 1), the majority (96.8%; n=106 712) of DMRs had lower

202   DNA methylation in the placenta (referred to as Hypo-DMRs) and only a small proportion

203   (3.2%; n=3 528) showed increased methylation levels (referred to as Hyper-DMRs) compared to

204   the embryo (Figure S2). For Hypo-DMRs, tiles mainly overlapped (96%; n=102 982) with

205   intergenic, intron, exon and promoter-TSS regions (Figure S2). For each of the genomic feature

206   categories of Hypo-DMRs, the average DNA methylation levels in the placenta were essentially

207   half of those present in the embryo (Figure 2B). As for DMRs with higher methylation levels in

208   the placenta (Hyper-DMRs), we noticed that the vast majority of these tiles (83%; n=2 929) had

209   very low methylation levels in the embryo (<20%) (Figure 2A-B). Most of Hyper-DMRs

210   overlapped intergenic, intron, exon and promoter-TSS regions (93%; n=3 272, Figure S2). We

211   then investigated the relationship between gene expression and DMR DNA methylation levels.

212   Highly expressed genes in placental tissue such as *Syna* (*Syncytin A*) (Mi et al., 2000) showed

213   overall lower methylation levels in the placenta when compared to the embryo (Figure 2D,

214   smoothed representation) (Hansen et al., 2012). Similar observations were made in the gene body

215   of *Atf6b* (*Activating Transcription Factor 6 Beta*), a gene implicated in the transcriptional

216   downregulation of *Pgf* (*Placental Growth Factor*) in response to endoplasmic reticulum stress in

217   pathological placentas (Mizuuchi et al., 2016). As for genes predominantly expressed in the

218   embryo, *Mir219a-2/Mir219b*, a brain-specific non-coding microRNA, showed higher

219   methylation in the placenta (Figure 2D). It was recently shown that *Mir219* was abnormally

220   expressed during pregnancy in amnion retrieved specifically from obese women (Nardelli et al.,

221   2014) and, interestingly, obesity has been suggested to cause epigenetic changes (Lillycrop and

222   Burdge, 2011). Another example of placenta Hyper-DMRs is *Sox6* (*SRY-Box 6*), which is

223   implicated in the terminal differentiation of muscle (Figure 2D) (Kamachi and Kondoh, 2013).

224   These observations point to an association between tissue-specific DNA methylation levels of

225   DMRs and biological functions. Gene ontology enrichment analyses further support that Hypo-

226   DMRs were strongly associated to germline functions and reproduction (*e.g.*, male and female

227   gamete generation, reproduction, piRNA metabolic process, meiotic cell cycle, germ cell

228   development) (Figure 2C). As for Hyper-DMRs, top biological processes were mostly associated

229   with developmental and differentiation processes (*e.g.*, regionalization, embryo development,

230   pattern specification process, skeletal system, head development) (Figure 2C). Fittingly, the

231   biological functions were completely divergent between Hypo- and Hyper-DMRs. Altogether,

232   these results denote that Hypo- and Hyper-DMRs are present across genomic features between

233   mid-gestation embryo and placenta, and that these DNA methylation divergences are implicated

234   in promoting/repressing specific processes during embryonic and placental development.

235

236   ***Presence of Distinctive DMR Categories between Mid-Gestation Embryo and Placenta***

237   Amongst DMRs, our analyses also suggest the presence of particular DMR categories

238   based on their level of DNA methylation in the embryo and placenta (Figure 2A). By defining

239   subsets of DMRs and establishing their dynamic properties between tissues, we might better

240   understand the genome-wide asymmetry in DNA methylation levels observed between the

241   embryo and the placenta. To do so, we first clustered DMR-associated tiles in 6 different

242   categories based on their range of low, mid and high methylation level (Low; <20%, Mid; ≥20 to

243   <80%, High; ≥80%) in the embryo and the placenta, and followed the DMR category transitions

244   between both tissues. We observed that DMRs with High-levels of methylation in the embryo

245   overlapped with a large proportion of DMRs that showed Mid-levels of methylation in the

246   placenta (Figure 3A,B; High-Mid n=72 715), whereas only a fraction corresponded to DMRs

247   with Low-levels of methylation in the placenta (Figure 3A,B; High-Low n=1 889). As for DMRs

248   with Mid-levels of methylation in embryo, the largest part remained in that same Mid-levels

249   category in the placenta (Figure 3A; Mid-Mid n=23 640). Nonetheless, a portion of these

250   embryonic Mid-levels DMRs were directed to DMRs with either Low- (Figure 3A; Mid-Low

251   n=9 055) or High- (Figure 3A; Mid-High n= 21) levels of methylation in the placenta. Finally,

252   DMRs with Low-levels of methylation in the embryo all showed Mid-levels of methylation in

253   the placenta (Figure 3A; Low-Mid n=2 920). Thus, when we subdivide our DMRs into

254   distinctive categories, we uncover that embryonic cells possess a large proportion of DMRs of

255   High-level (≥80%) of DNA methylation, which remain potentially static in embryonic tissues,

256   whereas the vast majority of these DMRs have inferior and wide-range DNA methylation levels

257   within placental tissue.

258

259   ***Specific Genomic Features Associated with DMR Categories***

9

260   We next aimed to determine if the genomic distribution of embryo-placenta DMR

261   categories was associated with distinct genomic features. First, by classifying by genomic

262   annotations, we observed that DMRs with reduced methylation levels in the placenta (High-Mid,

263   High-Low, Mid-Low) were prevailingly found in intergenic regions (>50% of tiles) (Figure 3C),

264   whereas DMR categories with equivalent (Mid-Mid) or superior methylation level (Mid-High,

265   Low-Mid) in the placenta were more frequent in genic associated regions (>50% of tiles).

266   However, divergence between DMR categories was observed when we performed ontology

267   analyses on promoter regions (Figure S3), as each DMR subtype clearly showed distinct

268   biological functions. For example, High-Mid DMRs top functions were related to genes (e.g.,

269   *Aszl, Tnp1*, *Piwil2*) associated with male gamete generation, piRNA metabolic process and male

270   meiotic nuclear division, whereas those of the Low-Mid category were mostly associated with

271   developmental aspects (e.g., skeletal system development, regionalization, nervous system

272   development). Since we know that in placenta, activation of retrotransposon-derived genes is

273   interrelated with low DNA methylation levels (Macaulay et al., 2011, Reiss et al., 2007, Cohen

274   et al., 2011), we next assessed how DMR categories overlapped with major types of

275   retrotransposons (LINE; long interspersed nuclear elements, SINE; short interspersed nuclear

276   element, and LTR; long terminal repeats). Out of the DMR categories, those with High-levels of

277   methylation in the embryo and either Mid- or Low-levels in the placenta (High-Mid and High-

278   Low) showed the most enriched overlap with retrotransposons, with 92% and 96% respectively

279   (Figure 3D). DMR categories associated with gain of methylation in the placenta (Mid-High and

280   Low-Mid) showed the least overlap with retrotransposons, especially the Low-Mid subtype. This

281   highlights that during the *de novo* acquisition of DNA methylation patterns, DMRs with High-

282   levels of methylation in the embryo and lower levels in the placenta are almost exclusively

283   within retrotransposons-associated sequences, whereas DMRs with Low-levels of methylation in

284   the embryo and higher DNA methylation in the placenta are preferentially outside

285   retrotransposons-associated sequences. Finally, we investigated the proximity of the DMR

286   categories in regards to CpG rich (CpG islands; CGI), neighbouring (shore; < 2kb away from

287   CGIs, shelf; 2-4kb away from CGIs) and distant (open sea; > 4kb away from CGIs) regions

288   (Figure 3E). We observed that most DMR categories are depleted from CGIs and are mostly

289   found in open sea regions. In contrast, ~60% of tiles in Low-Mid DMRs overlapped with CGI,

290   shores and shelves, revealing that the acquisition of *de novo* methylation for these genomic

10

291   fragments in the extraembryonic lineage preferentially targets sequences inside or surrounding

292   CGIs.

293   Altogether, these results indicate that the asymmetry within DMR categories, based on

294   their methylation levels in the embryo and the placenta, can be associated to specific biological

295   functions and genomic-derived features (e.g., CpG, retrotransposon contents). This is particularly

296   apparent for DMRs with High-levels in the embryo (High-Mid, High-Low) and those with higher

297   methylation levels in the placenta (Low-Mid).

298

299   ***DMR Categories are Established During the De Novo Methylation Wave and Maintained***

300   ***Throughout Development***

301   To gain insights into the kinetics of lineage-specific DMR establishment between mid-

302   gestation embryo and placenta, as well as their status during development, we assessed the levels

303   of methylation associated with tiles for each DMR category as a function of their developmental

304   stage. Publicly available sequencing data (Smith et al., 2012, Whidden et al., 2016) were

305   analyzed using our custom script to generate 100bp tiles, and the DNA methylation levels for

306   each tile were calculated. In E3.5 blastocysts, when the mouse genome is mostly depleted from

307   DNA methylation marks, we observed low global DNA methylation levels (average <20%) for

308   all DMR subtypes, with similar median levels between the committed cells of the inner cell mass

309   (ICM) and trophectoderm lineages (Figure 4). DNA methylation levels tended to be higher in the

310   trophectoderm for regions falling in the Mid-High DMRs, although measurements are based on

311   very few DMRs for this specific category (n=21, Figure 3B, Mid-High). Since global DNA

312   methylation is re-acquired in the next few subsequent developmental stages, we then asked

313   whether the contrast in DNA methylation levels associated with the various DMR categories at

314   mid-gestation would already be present between E6.5 epiblast and extraembryonic ectoderm

315   (ExE) cell lineages, layers that are mostly composed of homogeneous and undifferentiated cell

316   populations. For all DMR categories, DNA methylation levels in the E6.5 epiblast and ExE

317   already showed similar pattern trends to those observed in the E10.5 embryo and placenta

318   (Figure 4, Table S2). Interestingly, for all DMR categories we observed slightly higher DNA

319   methylation levels in E6.5 ExE compared to E10.5 placenta (Figure 4, Table S2). However,

320   when measured in the subsequent developmental stages (E10.5, E11.5, E15 and E18), levels

321   associated with each category stabilized and remained in the same methylation range. This is true

11

322 for all categories, except for the Mid-High DMRs where methylation levels are reduced by ~20%

323 at E18. As for the E6.5 epiblast DNA methylation profiles, they closely matched those observed

324 in the E10.5 embryo, except again for the Mid-High DMRs. For each of the DMR subtypes, the

325 DNA methylation levels were largely stable and persisted across other time points (E6.5, E10.5,

326 E11.5) in embryonic cells. Although no public DNA methylation data were available for whole

327 embryos at later stages, when we overlapped tiles associated with E10.5 DMR categories with

328 data from differentiated tissues of adult mice, the global DNA methylation profiles closely

329 matched those for the majority of DMR categories (High-Mid, High-Low, Mid-Mid and Mid-

330 Low) (Figure 4, Figure S4). We conclude that the various DMR categories observed at E10.5 are

331 established during the embryonic and extraembryonic lineage-specification processes occurring

332 during the peri-implantation wave of *de novo* methylation, and that these DNA methylation

333 landscapes are widely retained throughout embryo and placenta development. Furthermore, for

334 most DMR categories, the DNA methylation levels observed in developing embryos are long-

335 lasting and conserved throughout somatic cell differentiation.

336

Dnmt3a- or Dnmt3b-Deficiency Alters Proper Establishment of DMR-Associated Patterns

338 Since the combined activity of DNMT3A and DNMT3B is essential for proper

339 establishment of DNA methylation profiles and normal development, we next sought to define

340 the contribution of each enzyme in the *de novo* establishment of DNA methylation in subtypes of

341 DMRs in embryonic and extraembryonic cell lineages. To do so, we used DNA methylation data

342 from publicly available datasets (whole genome bisulfite sequencing and RRBS) at E6.5

343 (epiblast and ExE) and E8.5 (embryo) with various inactive forms of *Dnmts*. First, when we

344 overlapped our All-tiles subset, we observed a substantial reduction (p□0.0001) in average DNA

345 methylation in absence of DNMT3A (37.81%) or DNMT3B (31.48%) in the E6.5 epiblast

346 compared to wild-type (44.81%), whereas in the E6.5 ExE such a comparable loss was only

347 associated with a *Dnmt3b*-deficiency (wt: 34.38% vs *Dnmt3b*$^{-/-}$: 19.33%, p□0.0001) (Figure S5).

348 Similarly, in the E8.5 embryo, a significant reduction in average DNA methylation level was

349 measured with lack of *Dnmt3a* or *Dnmt3b* expression compared to wild-type (wt: 47.5%;

350 *Dnmt3a*$^{-/-}$: 43.6%; *Dnmt3b*$^{-/-}$: 34%, p□0.0001) (Figure S5). For most DMR subtypes, absence of

351 DNMT3A caused modest or no reduction on overall DNA methylation levels in E6.5 epiblast

352 and ExE (Figure 5A and S6, Table S3). Intriguingly, *Dnmt3a*-deficiency caused a slight gain of

12

353   methylation (wt: 76.9% vs $Dnmt3a^{-/-}$: 81.5%, p$\square$0.0001) level in the E6.5 epiblast for High-Mid

354   DMRs, suggesting a potential overcompensation effect by DNMT3B in the epiblast on this

355   specific DMR subtype. In comparison, *Dnmt3b*-depletion led to a substantial loss of average

356   methylation levels in all DMR categories in the E6.5 epiblast and ExE, except for epiblast High-

357   Mid DMRs (Figure 5A, Table S3) for which a compensatory mechanism provided high levels of

358   methylation (wt: 76.9% vs $Dnmt3b^{-/-}$: 71.6%). The compensatory mechanism on High-Mid

359   DMRs in response to *Dnmt3b*-deficiency was ineffective in the E6.5 ExE. When we focused on

360   promoter-TSS for each DMR categories, we observed again that loss of methylation for these

361   regulatory regions was principally associated with *Dnmt3b*-deficiency (Figure 5B). The

362   promoter-TSS regions associated with High-Mid DMRs retained relatively high methylation

363   levels for either $Dnmt3a^{-/-}$ or $Dnmt3b^{-/-}$ epiblast samples, demonstrating a robust and

364   compensatory *de novo* methylation mechanism. To further underline the impact of DNMT3A or

365   DNMT3B on the *de novo* methylation of DMRs, we measured methylation levels for DMRs

366   selected from our gene enrichment analyses (*Fgb*, *P2rx7*, *Pcyt2*, *Etnppl*, *Ralgds*, *Lrp5*) and other

367   genomic segments covered by multiple tiles (*Cxxc1*, *Fcgrt*, *Lamp5*, *Mbd1*, *Lphn1*, *Pick1*, *Irf1*)

368   (Figure S7 & S8) in *Dnmt3a*- or *Dnmt3b*-deficient epiblast and ExE. In line with our global

369   observations, for most DMR-associated tiles, a *Dnmt3b*-deficiency in E6.5 epiblast or ExE

370   caused a more severe loss of methylation compared to lack of *Dnmt3a*. However, for some

371   regions in the E6.5 epiblast (e.g., *Pick1*, *Irf1*), $Dnmt3a^{-/-}$ methylation levels were inferior to those

372   of $Dnmt3b^{-/-}$. Noteworthy, for most DMRs, lack of co-factor *Dnmt3l* affected DNA methylation

373   levels to greater extent than *Dnmt3a*-deficiency (Figure S6). Overall, we show that of DNMT3A

374   and DNMT3B participate in the establishment of the asymmetric methylation patterns associated

375   with the various DMR categories in both embryonic and extraembryonic cells, with DNMT3B

376   being the principal contributor in both cell lineages during the *de novo* reprogramming wave as it

377   can compensate almost entirely for the absence of DNMT3A.

378

379   ***Decline in Compensatory DNA Methylation Mechanisms in Response to Dnmt3a- or Dnmt3b-***

380   ***Deficiency.***

381   As embryonic development progresses from E6.5 to E8.5, our data suggest that lack of

382   DNMT3A or DNMT3B further reduces global methylation levels of DMRs (High-Mid, High-

383   Low, Mid-Low and Mid-Mid), evoking that absence of either enzymatic activity causes an

384   additive and extended effect (Figure 5A-B). To further define the robustness in compensatory

385   mechanism between DNMT3A or DNMT3B in the establishment and maintenance of DNA

386   methylation on DMRs categories, we focused on High-Mid promoter-TSS- associated DMRs as

387   they have the highest DNA methylation levels and require the most *de novo* methyltransferase

388   activity. Methylation differences of ≥20% between wild-type and *Dnmt3a-* or *Dnmt3b*-deficient

389   samples were considered as regions showing substantial lack of compensation. In agreement

390   with our results (Figure 5A-B), we observed that at E6.5, DNMT3B can compensate almost

391   entirely for DNMT3 Aloss by maintaining methylation levels on most promoters-TSS associated

392   tiles in the epiblast (410/437 = 93.8%) and ExE (558/602 = 92.7%), whereas DNMT3A can only

393   partially alleviate the lack of DNMT3B in the epiblast (315/410 = 78.6%) and ExE (244/524 =

394   46.6%) (Figure 6A-B). As embryonic cell lineages development evolves between E6.5 and E8.5,

395   global methylation levels increase on promoter-TSS of High-Mid DMRs. However, we detected

396   a sharp decline in the compensatory mechanism to rescue the *de novo* and/or maintenance of

397   methylation levels of promoter-TSS DMRs in the *Dnmt3a-* (524/627 = 80.9%) or *Dnmt3b-*

398   (256/622 = 41.2%) deficient E8.5 embryos. This is further highlighted when we focus on a

399   subgroup of 314 promoter-TSS associated tiles overlapping all of 9 data sets (Figure 6C),

400   including gene promoters (e.g., *Asz1, Catsper1, Ccdc42, Dmrtb1, Piwil2, Rpl10l, Sox30, Sycp1,*

401   *Tnp1, Ttll1, Zfn42*) related to our top enriched biological functions (i.e., piRNA, gamete

402   generation and germ cells, meiotic nuclear division). Although E8.5 *Dnmt3a-* or *Dnmt3b-*

403   deficient ExE data was not available, our data suggest that greater compensation failure would

404   also be observed in this tissue. Thus, embryonic-placental DMRs need the combined action of

405   DNMT3Aand DNMT3Bto both establish and maintain proper asymmetric levels during early

406   development as compensatory DNA methylation mechanisms during the *de novo* wave of

407   methylation decline overtime and fail to overcome methyltransferase shortage in later

408   development stages.

409

410   **DISCUSSION**

411   With recent breakthroughs in high-throughput sequencing, we now have a better

412   understanding of the dynamic of DNA methylation erasure occurring in early cleavage stage

413   embryos following fertilization. However, the discrepancies in acquisition of genome-wide DNA

414   methylation patterns in early post-implantation embryonic and extraembryonic cell lineages

415   remain to be methodically delineated. To address this issue and further our understanding of the

416   DNA methylation asymmetry that guides the developmental trajectory of embryonic and

417   extraembryonic cell lineages, we established genome-wide DNA methylation profiles of mouse

418   embryo and placenta at mid-gestation, and analyzed various publicly available developmental

419   stage specific embryo and placenta DNA methylation datasets. Using this strategy, we uncovered

420   that 45% of the genomic regions analyzed differ in DNA methylation status (≥20%) between

421   mid-gestation embryo and placenta, and that these DMRs can be further divided into categories

422   based on their levels of DNA methylation (Low; <20%, Mid; ≥20 to <80%, High; ≥80%) in the

423   embryo and placenta. We show that the embryo and placenta acquire specific DMR categories

424   during the early stage of the *de novo* DNA methylation wave, and that these DMRs persist

425   throughout prenatal development, as well as into somatic adult tissues. Furthermore, we show

426   that *Dnmt3b* primarily drives the divergence in DNA methylation levels associated with these

427   specific DMRs and that *de novo* methyltransferase activity of *Dnmt3b* can almost entirely

428   compensate for lack of *Dnmt3a* in the asymmetric establishment of embryonic and placental

429   DMRs, but that *Dnmt3a* can only partially palliate the absence of *Dnmt3b*. However, with

430   developmental progression, this compensatory DNA methylation mechanism becomes less

431   effective.

432   Our results indicate that the kinetics of DNA methylation acquisition leading to specific

433   embryo-placenta DMR categories is not a stepwise process occurring throughout cell fate

434   decisions and patterning of embryonic and extraembryonic lineages, but a prompt progression in

435   the early post-implanted conceptus. These results are in line with studies reflecting that the

436   initiation of asymmetric DNA methylation levels begins within the trophoblast and the inner cell

437   mass of the blastocyst (Santos et al., 2002), and becomes highly evident by the time the epiblast

438   acquires its initial global DNA methylation patterns at E6.5 during the *de novo* reprogramming

439   wave (Auclair et al. 2014, Smith et al. 2017). Our results show that the acquisition period

440   between E4.5 and E6.5 is particularly key to establishing asymmetric DNA methylation patterns

441   associated with mid-gestation embryo-placenta DMR classes, and that these DMR associated-

442   patterns are long-lasting across stages of prenatal development. Since we studied cell populations

443   derived from embryonic and placental tissues, we cannot dismiss the prevalence of cell-to-cell

444   heterogeneity in the acquisition kinetics of specific DMR patterns. Despite this concern, our

445   results indicate that embryonic cells have a large body of DMRs with High-levels (≥80%) and

15

446   Low-levels (<20%) of methylation that remain static across development, as well as in somatic
447   cell types (High-Mid & High-Low DMRs), whereas compared to the embryo, the placental
448   DMRs have overall lower methylation levels and are more broadly distributed amongst
449   methylation levels, which has also been shown in other studies where genome-wide DNA
450   methylation profiles of placental cells were compared to other tissues and specific cell types
451   (Schroeder et al., 2013; Chatterjee et al., 2016; Smith et al., 2017). Lower methylation levels in
452   the placenta have been associated with reduced *de novo* methyltransferase activity in the ExE
453   during the *de novo* reprogramming wave (Fulka et al., 2004, Santos et al., 2002). Nevertheless,
454   we observe methylation level peaks for all DMR categories within the ExE at E6.5 before levels
455   stabilize at E10.5. As of now, the implication of these methylation level peaks on future
456   regulation mechanisms and methylation profiles is unknown. Moreover, it remains to be
457   determined whether global reduction in DNA methylation marks on DMRs between the E6.5 and
458   E10.5 extraembryonic cell lineages is stochastic or targeted, and whether it occurs through
459   passive or active mechanisms.

460   We also observed an enrichment of retrotransposons (i.e., LINE, SINE, LTR) in DMRs
461   especially in those with High-levels of methylation in the embryo and lower-levels in the
462   placenta, whereas DMRs with Low-levels of methylation in the embryo and higher levels in the
463   placenta are preferentially outside retrotransposons-associated sequences. Earlier findings of
464   Chapman et *al.* (Chapman et al., 1984) revealed that repeat regions in the placenta appear to lack
465   tight control of their methylation patterns, perhaps indicating that maintaining methylation, and
466   therefore repression of these elements for genome stability and integrity, is not critical given the
467   relatively short lifespan of this organ. However, we do observe Mid-range methylation levels
468   (20-80%) in the placenta for a substantial portion of DMRs that are associated with
469   retrotransposons, revealing that specific genomic regions associated with repetitive elements do
470   need tight regulation in extraembryonic cell lineages for proper development. These results are in
471   line with findings exposing that the deletion of genome-defense gene *Tex19.1* leads to the de-
472   repression of LINE1 and compromises placental development, suggesting that disparities
473   between retrotransposon suppression and genome-defense mechanisms might contribute to
474   placenta dysfunction and disease (Reichmann et al., 2013).

475   DNMT3A and DNMT3B are required to establish proper methylation profiles on the
476   embryonic genome during the *de novo* reprogramming wave, as both methyltransferase enzymes

16

477   have redundant, but also specific functions. However, the activity of DNMT3B is the main

478   contributor in the acquisition of profiles in epiblast cells, and especially commands methylation

479   on CGIs associated with developmental genes (Auclair et al., 2014). Auclair et *al*. highlighted

480   that in the absence of DNMT3B, DNMT3A was not able to counterbalance, leading to the loss of

481   promoter-CGI methylation and gain of expression of germline genes (e.g., *Sycp1*, *Sycp2*, *Mael*,

482   *Rpl10l*, *Dmrtb1*) in somatic cells of the embryo. Here, we show that the promoter of these

483   germline genes, associated with meiotic and piRNA processes as well as other genes with similar

484   biological functions, are highly enriched in High-Mid DMRs. We also reveal that for this

485   particular set of High-Mid DMRs, mainly deprived of CGIs, DNMT3A is able to substantially

486   counterbalance the lack of DNMT3B in the E6.5 epiblast and establish global DNA methylation

487   levels, whereas in the ExE, this compensatory mechanism is rather inefficient. Globally, we

488   show that DNMT3B is much more potent at compensating than DNMT3A in both the epiblast

489   and ExE for all DMR categories, indicating that DNMT3B is the main *de novo* enzyme driving

490   asymmetric DNA methylation patterns between the embryo and placenta. Although

491   compensatory mechanisms have been observed in *Dnmt3a* or *Dnmt3b*-depleted conceptuses, we

492   still do not fully understand the process as *Dnmt3a* and *Dnmt3b* have cell lineage specific

493   expression during the peri-implantation developmental period. As development progresses, we

494   observed that the compensation mechanism in *Dnmt3a* or *Dnmt3b*-deficient embryos remains

495   apparent at E8.5 on most DMR categories, but is less effective as the methylation gaps increase

496   compared to wild-type. This correlates with a developmental period where DNMT3A is now the

497   main *de novo* methyltransferase enzyme in both the embryo and placenta (Okano et al., 1999,

498   Watanabe et al., 2002), and with a compensatory activity of DNMT3A being less effective. This

499   suggests that DNMT3B activity is critical to ensure proper establishment of DNA methylation

500   asymmetry between the embryonic and extraembryonic cell lineages during the *de novo*

501   reprogramming wave, but that DNMT3A is required during the developmental progression to

502   safeguard methylation levels on DMR categories.

503

504   **CONCLUSION**

505   We demonstrate that asymmetry between embryo and placenta DNA methylation patterns

506   occurs rapidly during *de novo* acquisition of methylation marks in the early post-implanted

507   conceptus, and that these patterns are long-lasting across subtypes of DMRs. We also reveal that

508   at the peri-implantation stages, *de novo* methyltransferase activity of DNMT3B is the main

509   provider of asymmetric methylation marks on DMRs, and that it largely palliates the lack of

510   DNMT3A in the epiblast and ExE. However, as development progresses, DNMT3A becomes the

511   principal *de novo* methyltransferase by mid-gestation, and DNMT3B methyltransferase activity

512   is less effective at promoting compensation. These results further underline why embryos

513   developing without DNMT3B have severe DNA methylation defects and die at mid-gestation,

514   whereas those without DNMT3A only die postnatally. Further investigation is required to

515   determine the molecular mechanisms controlling the precise *de novo* acquisition of long-lasting

516   methylation marks on specific DMR subtypes in the embryonic and extraembryonic cell

517   lineages, and how errors in this process could lead to abnormal development and diseases.

518

519

523

524   **COMPETING INTERESTS**

525   No competing interests declared

526

532

533   **DATA AVAILABILITY**

534   The data from this study have been submitted to the Gene Expression Omnibus (#GSE95610).

535   Reviewer link:

536 https://www.ncbi.nlm.nih.gov/geo/query/acc.cgi?token=ghsnmqoctlgjlcj&acc=GSE95610

537

538 **Table S1. Annotation and DNA methylation values associated with DMRs.**

539 **Table S2. DNA methylation levels for DMR categorises across development.**

540 **Table S3. DNA methylation levels for DMR categories in various *Dnmt* knockout mouse**
541 **models.**

542 **Table S4. Number of 100bp tiles in each category of public data that overlap with Embryo-**
543 **Placenta DMRs (related to Figure 4; 5A; S4; S5; S6)**

544

545 **REFERENCES**

546 AKALIN, A., KORMAKSSON, M., LI, S., GARRETT-BAKELMAN, F. E., FIGUEROA, M.
547   E., MELNICK, A. & MASON, C. E. 2012. methylKit: a comprehensive R package for
548   the analysis of genome-wide DNA methylation profiles. *Genome Biol,* 13**,** R87.
549 AUCLAIR, G., GUIBERT, S., BENDER, A. & WEBER, M. 2014. Ontogeny of CpG island
550   methylation and specificity of DNMT3 methyltransferases during embryonic
551   development in the mouse. *Genome Biol,* 15**,** 545.
552 BESTOR, T. H. 2000. The DNA methyltransferases of mammals. *Hum Mol Genet,* 9**,** 2395-402.
553 BOYLE, P., CLEMENT, K., GU, H., SMITH, Z. D., ZILLER, M., FOSTEL, J. L., HOLMES,
554   L., MELDRIM, J., KELLEY, F., GNIRKE, A. & MEISSNER, A. 2012. Gel-free
555   multiplexed reduced representation bisulfite sequencing for large-scale DNA methylation
556   profiling. *Genome Biol,* 13**,** R92.
557 CHAPMAN, V., FORRESTER, L., SANFORD, J., HASTIE, N. & ROSSANT, J. 1984. Cell
558   lineage-specific undermethylation of mouse repetitive DNA. *Nature,* 307**,** 284-6.
559 CHATTERJEE, A., MACAULAY, E. C., RODGER, E. J., STOCKWELL, P. A., PARRY, M.
560   F., ROBERTS, H. E., SLATTER, T. L., HUNG, N. A., DEVENISH, C. J. & MORISON,
561   I. M. 2016. Placental Hypomethylation Is More Pronounced in Genomic Loci Devoid of
562   Retroelements. *G3 (Bethesda),* 6**,** 1911-21.
563 CHUONG, E. B. 2013. Retroviruses facilitate the rapid evolution of the mammalian placenta.
564   *Bioessays,* 35**,** 853-61.
565 CHURCH, D. M., GOODSTADT, L., HILLIER, L. W., ZODY, M. C., GOLDSTEIN, S., SHE,
566   X., BULT, C. J., AGARWALA, R., CHERRY, J. L., DICUCCIO, M., HLAVINA, W.,
567   KAPUSTIN, Y., MERIC, P., MAGLOTT, D., BIRTLE, Z., MARQUES, A. C.,
568   GRAVES, T., ZHOU, S., TEAGUE, B., POTAMOUSIS, K., CHURAS, C., PLACE, M.,
569   HERSCHLEB, J., RUNNHEIM, R., FORREST, D., AMOS-LANDGRAF, J.,
570   SCHWARTZ, D. C., CHENG, Z., LINDBLAD-TOH, K., EICHLER, E. E., PONTING,
571   C. P. & MOUSE GENOME SEQUENCING, C. 2009. Lineage-specific biology revealed
572   by a finished genome assembly of the mouse. *PLoS Biol,* 7**,** e1000112.
573 COHEN, C. J., REBOLLO, R., BABOVIC, S., DAI, E. L., ROBINSON, W. P. & MAGER, D.
574   L. 2011. Placenta-specific expression of the interleukin-2 (IL-2) receptor beta subunit
575   from an endogenous retroviral promoter. *J Biol Chem,* 286**,** 35543-52.

19

576   CROSS, J. C. 2000. Genetic insights into trophoblast differentiation and placental
577   morphogenesis. *Semin Cell Dev Biol,* 11**,** 105-13.
578   CROSS, J. C., WERB, Z. & FISHER, S. J. 1994. Implantation and the placenta: key pieces of
579   the development puzzle. *Science,* 266**,** 1508-18.
580   DECATO, B. E., LOPEZ-TELLO, J., SFERRUZZI-PERRI, A. N., SMITH, A. D. & DEAN, M.
581   D. 2017. DNA Methylation Divergence and Tissue Specialization in the Developing
582   Mouse Placenta. *Mol Biol Evol,* 34**,** 1702-1712.
583   EMERA, D. & WAGNER, G. P. 2012. Transposable element recruitments in the mammalian
584   placenta: impacts and mechanisms. *Brief Funct Genomics,* 11**,** 267-76.
585   FULKA, H., MRAZEK, M., TEPLA, O. & FULKA, J., JR. 2004. DNA methylation pattern in
586   human zygotes and developing embryos. *Reproduction,* 128**,** 703-8.
587   GU, H., SMITH, Z. D., BOCK, C., BOYLE, P., GNIRKE, A. & MEISSNER, A. 2011.
588   Preparation of reduced representation bisulfite sequencing libraries for genome-scale
589   DNA methylation profiling. *Nat Protoc,* 6**,** 468-81.
590   GUO, H., ZHU, P., YAN, L., LI, R., HU, B., LIAN, Y., YAN, J., REN, X., LIN, S., LI, J., JIN,
591   X., SHI, X., LIU, P., WANG, X., WANG, W., WEI, Y., LI, X., GUO, F., WU, X., FAN,
592   X., YONG, J., WEN, L., XIE, S. X., TANG, F. & QIAO, J. 2014. The DNA methylation
593   landscape of human early embryos. *Nature,* 511**,** 606-10.
594   HAIG, D. 2012. Retroviruses and the placenta. *Curr Biol,* 22**,** R609-13.
595   HANSEN, K. D., LANGMEAD, B. & IRIZARRY, R. A. 2012. BSmooth: from whole genome
596   bisulfite sequencing reads to differentially methylated regions. *Genome Biol,* 13**,** R83.
597   HIRASAWA, R., CHIBA, H., KANEDA, M., TAJIMA, S., LI, E., JAENISCH, R. & SASAKI,
598   H. 2008. Maternal and zygotic Dnmt1 are necessary and sufficient for the maintenance of
599   DNA methylation imprints during preimplantation development. *Genes Dev,* 22**,** 1607-
600   16.
601   HON, G. C., RAJAGOPAL, N., SHEN, Y., MCCLEARY, D. F., YUE, F., DANG, M. D. &
602   REN, B. 2013. Epigenetic memory at embryonic enhancers identified in DNA
603   methylation maps from adult mouse tissues. *Nat Genet,* 45**,** 1198-206.
604   HOWELL, C. Y., BESTOR, T. H., DING, F., LATHAM, K. E., MERTINEIT, C., TRASLER, J.
605   M. & CHAILLET, J. R. 2001. Genomic imprinting disrupted by a maternal effect
606   mutation in the Dnmt1 gene. *Cell,* 104**,** 829-38.
607   KAMACHI, Y. & KONDOH, H. 2013. Sox proteins: regulators of cell fate specification and
608   differentiation. *Development,* 140**,** 4129-44.
609   KANEDA, M., OKANO, M., HATA, K., SADO, T., TSUJIMOTO, N., LI, E. & SASAKI, H.
610   2004. Essential role for de novo DNA methyltransferase Dnmt3a in paternal and maternal
611   imprinting. *Nature,* 429**,** 900-3.
612   KATO, Y., KANEDA, M., HATA, K., KUMAKI, K., HISANO, M., KOHARA, Y., OKANO,
613   M., LI, E., NOZAKI, M. & SASAKI, H. 2007. Role of the Dnmt3 family in de novo
614   methylation of imprinted and repetitive sequences during male germ cell development in
615   the mouse. *Hum Mol Genet,* 16**,** 2272-80.
616   LEGAULT, L.-M., CHAN, D. & MCGRAW, S. 2019. Rapid Multiplexed Reduced
617   Representation Bisulfite Sequencing Library Prep (rRRBS). *BIO-PROTOCOL,* 9.
618   LEI, H., OH, S. P., OKANO, M., JUTTERMANN, R., GOSS, K. A., JAENISCH, R. & LI, E.
619   1996. De novo DNA cytosine methyltransferase activities in mouse embryonic stem
620   cells. *Development,* 122**,** 3195-205.

621   LEONHARDT, H., PAGE, A. W., WEIER, H. U. & BESTOR, T. H. 1992. A targeting sequence
622   directs DNA methyltransferase to sites of DNA replication in mammalian nuclei. *Cell,*
623   71**,** 865-73.
624   LI, E. 2002. Chromatin modification and epigenetic reprogramming in mammalian development.
625   *Nat Rev Genet,* 3**,** 662-73.
626   LI, E., BESTOR, T. H. & JAENISCH, R. 1992. Targeted mutation of the DNA
627   methyltransferase gene results in embryonic lethality. *Cell,* 69**,** 915-26.
628   LILLYCROP, K. A. & BURDGE, G. C. 2011. The effect of nutrition during early life on the
629   epigenetic regulation of transcription and implications for human diseases. *J Nutrigenet*
630   *Nutrigenomics,* 4**,** 248-60.
631   MACAULAY, E. C., WEEKS, R. J., ANDREWS, S. & MORISON, I. M. 2011.
632   Hypomethylation of functional retrotransposon-derived genes in the human placenta.
633   *Mamm Genome,* 22**,** 722-35.
634   MAGNUS, N., GARNIER, D., MEEHAN, B., MCGRAW, S., LEE, T. H., CARON, M.,
635   BOURQUE, G., MILSOM, C., JABADO, N., TRASLER, J., PAWLINSKI, R.,
636   MACKMAN, N. & RAK, J. 2014. Tissue factor expression provokes escape from tumor
637   dormancy and leads to genomic alterations. *Proc Natl Acad Sci U S A,* 111**,** 3544-9.
638   MCGRAW, S., ZHANG, J. X., FARAG, M., CHAN, D., CARON, M., KONERMANN, C.,
639   OAKES, C. C., MOHAN, K. N., PLASS, C., PASTINEN, T., BOURQUE, G.,
640   CHAILLET, J. R. & TRASLER, J. M. 2015. Transient DNMT1 suppression reveals
641   hidden heritable marks in the genome. *Nucleic Acids Res*.
642   MI, S., LEE, X., LI, X., VELDMAN, G. M., FINNERTY, H., RACIE, L., LAVALLIE, E.,
643   TANG, X. Y., EDOUARD, P., HOWES, S., KEITH, J. C., JR. & MCCOY, J. M. 2000.
644   Syncytin is a captive retroviral envelope protein involved in human placental
645   morphogenesis. *Nature,* 403**,** 785-9.
646   MIZUUCHI, M., CINDROVA-DAVIES, T., OLOVSSON, M., CHARNOCK-JONES, D. S.,
647   BURTON, G. J. & YUNG, H. W. 2016. Placental endoplasmic reticulum stress
648   negatively regulates transcription of placental growth factor via ATF4 and ATF6beta:
649   implications for the pathophysiology of human pregnancy complications. *J Pathol,* 238**,**
650   550-61.
651   MONK, M. 1987. Genomic imprinting. Memories of mother and father. *Nature,* 328**,** 203-4.
652   MORGAN, H. D., SANTOS, F., GREEN, K., DEAN, W. & REIK, W. 2005. Epigenetic
653   reprogramming in mammals. *Hum Mol Genet,* 14 Spec No 1**,** R47-58.
654   NAKANISHI, M. O., HAYAKAWA, K., NAKABAYASHI, K., HATA, K., SHIOTA, K. &
655   TANAKA, S. 2012. Trophoblast-specific DNA methylation occurs after the segregation
656   of the trophectoderm and inner cell mass in the mouse periimplantation embryo.
657   *Epigenetics,* 7**,** 173-82.
658   NARDELLI, C., IAFFALDANO, L., FERRIGNO, M., LABRUNA, G., MARUOTTI, G. M.,
659   QUAGLIA, F., CAPOBIANCO, V., DI NOTO, R., DEL VECCHIO, L., MARTINELLI,
660   P., PASTORE, L. & SACCHETTI, L. 2014. Characterization and predicted role of the
661   microRNA expression profile in amnion from obese pregnant women. *Int J Obes (Lond),*
662   38**,** 466-9.
663   ODA, M., OXLEY, D., DEAN, W. & REIK, W. 2013. Regulation of lineage specific DNA
664   hypomethylation in mouse trophectoderm. *PLoS One,* 8**,** e68846.

665 OKAHARA, G., MATSUBARA, S., ODA, T., SUGIMOTO, J., JINNO, Y. & KANAYA, F.
666   2004. Expression analyses of human endogenous retroviruses (HERVs): tissue-specific
667   and developmental stage-dependent expression of HERVs. *Genomics,* 84**,** 982-90.
668 OKANO, M., BELL, D. W., HABER, D. A. & LI, E. 1999. DNA methyltransferases Dnmt3a
669   and Dnmt3b are essential for de novo methylation and mammalian development. *Cell,*
670   99**,** 247-57.
671 PICHE, J., GOSSET, N., LEGAULT, L. M., PACIS, A., ONEGLIA, A., CARON, M.,
672   CHETAILLE, P., BARREIRO, L., LIU, D., QI, X., NATTEL, S., LECLERC, S.,
673   BRETON-LARRIVEE, M., MCGRAW, S. & ANDELFINGER, G. 2019. Molecular
674   Signature of CAID Syndrome: Noncanonical Roles of SGO1 in Regulation of TGF-beta
675   Signaling and Epigenomics. *Cell Mol Gastroenterol Hepatol,* 7**,** 411-431.
676 PRICE, E. M., COTTON, A. M., PENAHERRERA, M. S., MCFADDEN, D. E., KOBOR, M. S.
677   & ROBINSON, W. 2012. Different measures of "genome-wide" DNA methylation
678   exhibit unique properties in placental and somatic tissues. *Epigenetics,* 7**,** 652-63.
679 REICHMANN, J., REDDINGTON, J. P., BEST, D., READ, D., OLLINGER, R., MEEHAN, R.
680   R. & ADAMS, I. R. 2013. The genome-defence gene Tex19.1 suppresses LINE-1
681   retrotransposons in the placenta and prevents intra-uterine growth retardation in mice.
682   *Hum Mol Genet,* 22**,** 1791-806.
683 REISS, D., ZHANG, Y. & MAGER, D. L. 2007. Widely variable endogenous retroviral
684   methylation levels in human placenta. *Nucleic Acids Res,* 35**,** 4743-54.
685 ROBINSON, W. P. & PRICE, E. M. 2015. The human placental methylome. *Cold Spring Harb*
686   *Perspect Med,* 5**,** a023044.
687 ROSSANT, J. & CROSS, J. C. 2001. Placental development: lessons from mouse mutants. *Nat*
688   *Rev Genet,* 2**,** 538-48.
689 SANTOS, F., HENDRICH, B., REIK, W. & DEAN, W. 2002. Dynamic reprogramming of DNA
690   methylation in the early mouse embryo. *Dev Biol,* 241**,** 172-82.
691 SCHROEDER, D. I., BLAIR, J. D., LOTT, P., YU, H. O., HONG, D., CRARY, F.,
692   ASHWOOD, P., WALKER, C., KORF, I., ROBINSON, W. P. & LASALLE, J. M. 2013.
693   The human placenta methylome. *Proc Natl Acad Sci U S A,* 110**,** 6037-42.
694 SENNER, C. E., KRUEGER, F., OXLEY, D., ANDREWS, S. & HEMBERGER, M. 2012.
695   DNA methylation profiles define stem cell identity and reveal a tight embryonic-
696   extraembryonic lineage boundary. *Stem Cells,* 30**,** 2732-45.
697 SHAFFER, B., MCGRAW, S., XIAO, S. C., CHAN, D., TRASLER, J. & CHAILLET, J. R.
698   2015. The dnmt1 intrinsically disordered domain regulates genomic methylation during
699   development. *Genetics,* 199**,** 533-41.
700 SLOTKIN, R. K. & MARTIENSSEN, R. 2007. Transposable elements and the epigenetic
701   regulation of the genome. *Nat Rev Genet,* 8**,** 272-85.
702 SMITH, Z. D., CHAN, M. M., HUMM, K. C., KARNIK, R., MEKHOUBAD, S., REGEV, A.,
703   EGGAN, K. & MEISSNER, A. 2014. DNA methylation dynamics of the human
704   preimplantation embryo. *Nature,* 511**,** 611-5.
705 SMITH, Z. D., CHAN, M. M., MIKKELSEN, T. S., GU, H., GNIRKE, A., REGEV, A. &
706   MEISSNER, A. 2012. A unique regulatory phase of DNA methylation in the early
707   mammalian embryo. *Nature,* 484**,** 339-44.
708 SMITH, Z. D., SHI, J., GU, H., DONAGHEY, J., CLEMENT, K., CACCHIARELLI, D.,
709   GNIRKE, A., MICHOR, F. & MEISSNER, A. 2017. Epigenetic restriction of
710   extraembryonic lineages mirrors the somatic transition to cancer. *Nature,* 549**,** 543-547.

711 WARREN, I. A., NAVILLE, M., CHALOPIN, D., LEVIN, P., BERGER, C. S., GALIANA, D.
712   & VOLFF, J. N. 2015. Evolutionary impact of transposable elements on genomic
713   diversity and lineage-specific innovation in vertebrates. *Chromosome Res,* 23**,** 505-31.
714 WATANABE, D., SUETAKE, I., TADA, T. & TAJIMA, S. 2002. Stage- and cell-specific
715   expression of Dnmt3a and Dnmt3b during embryogenesis. *Mech Dev,* 118**,** 187-90.
716 WHIDDEN, L., MARTEL, J., RAHIMI, S., RICHARD CHAILLET, J., CHAN, D. &
717   TRASLER, J. M. 2016. Compromised oocyte quality and assisted reproduction
718   contribute to sex-specific effects on offspring outcomes and epigenetic patterning. *Hum*
719   *Mol Genet*.
720 XIE, M., HONG, C., ZHANG, B., LOWDON, R. F., XING, X., LI, D., ZHOU, X., LEE, H. J.,
721   MAIRE, C. L., LIGON, K. L., GASCARD, P., SIGAROUDINIA, M., TLSTY, T. D.,
722   KADLECEK, T., WEISS, A., O'GEEN, H., FARNHAM, P. J., MADDEN, P. A.,
723   MUNGALL, A. J., TAM, A., KAMOH, B., CHO, S., MOORE, R., HIRST, M.,
724   MARRA, M. A., COSTELLO, J. F. & WANG, T. 2013. DNA hypomethylation within
725   specific transposable element families associates with tissue-specific enhancer landscape.
726   *Nat Genet,* 45**,** 836-41.
727 ZHOU, Y., ZHOU, B., PACHE, L., CHANG, M., KHODABAKHSHI, A. H., TANASEICHUK,
728   O., BENNER, C. & CHANDA, S. K. 2019. Metascape provides a biologist-oriented
729   resource for the analysis of systems-level datasets. *Nat Commun,* 10**,** 1523.
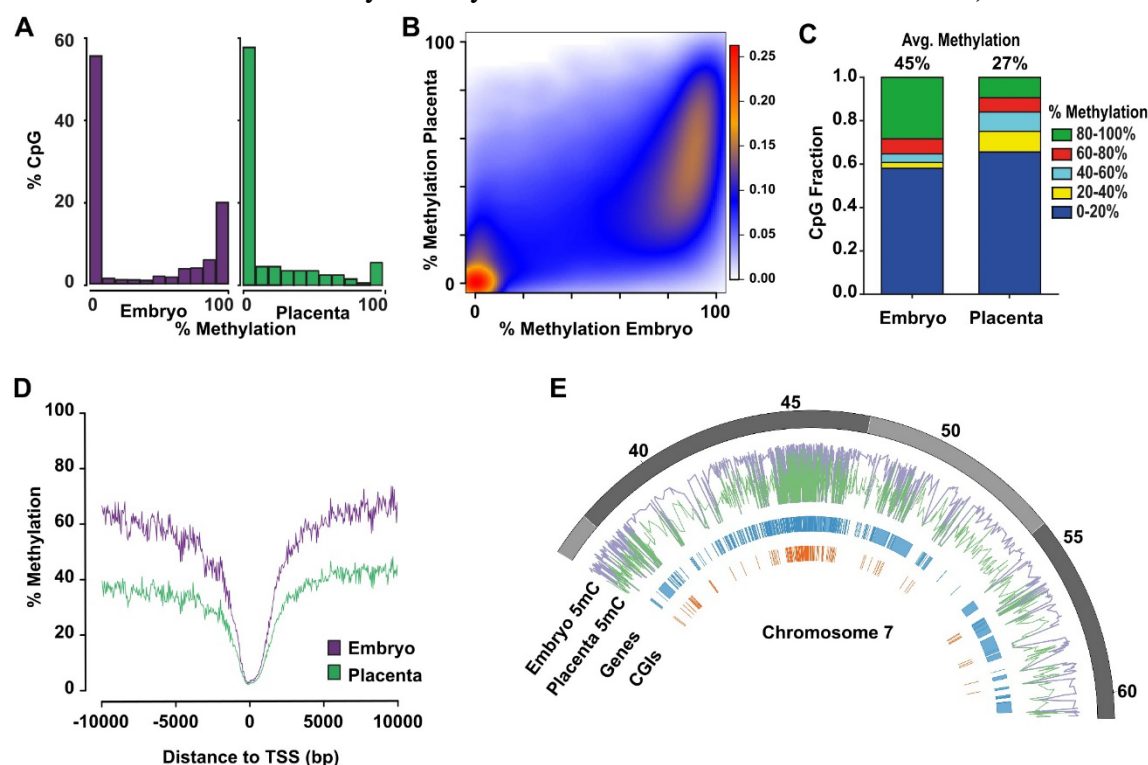

730
731
Figure 1. Distinctive patterns of genome-wide DNA methylation accumulation between mid-gestation embryo and placenta. Analyses of genome-wide DNA methylation sequencing results for embryo (n=4) and placenta (n=4). **A)** Density histograms showing the distribution of CpG methylation levels for embryo (*purple*) and placenta (*green*). **B)** Pairwise comparison of CpG methylation between embryo and placenta. Density increases from blue to red. **C)** CpG fraction of 100 bp tiles within 0-20%, 20-40%, 40-60%, 60-80% and 80-100% ranges in embryo

23

738   and placenta. Shown above bars, is the average CpG methylation for each unique tile represented
739   in graph. **D)** DNA methylation means surrounding the transcription start site (TSS) for All-tiles
740   in each experimental group. **E)** Circle plot showing methylation average of embryo (*purple*) and
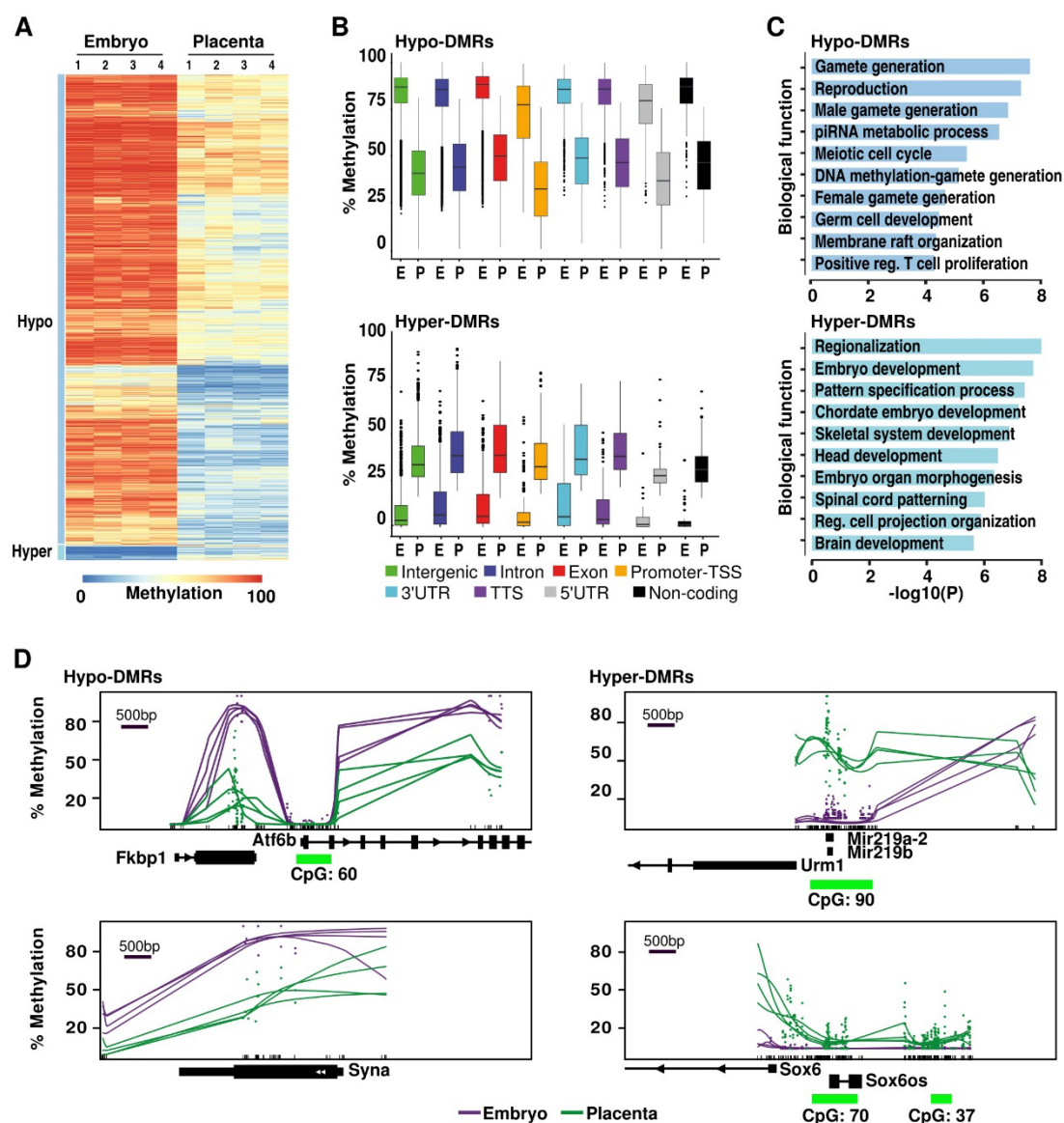741   placenta (*green*) across a portion of chromosome 7.

742
743
744
745
746
747
748
749

750
751
752   **Figure 2. Genome-wide methylation asymmetry across genomic features between embryo**
753   **and placenta**. Analyses of genome-wide DNA methylation sequencing results for embryo (n=4)

754 and placenta (n=4) samples. **A)** Heatmap representation of DNA methylation levels for the
755 20 000 tiles with the most variable levels between embryo and placenta (DNA methylation
756 variance >20% and *P*<0.05). **B)** Box-plots representing DNA methylation distribution in embryo
757 and placenta for the different genomic annotation regions (intergenic, intron, exon, promoter-
758 TSS, 3′UTR, TTS, 5′UTR and non-coding). **C)** Summary of biological functions associated with
759 promoter regions in Hypo- and Hyper-DMRs. **D)** Examples of smoothed methylation profiles
760 (*BSmooth* tool) in regions with lower methylation profiles (*Atf6b,* and *Syna*) or higher
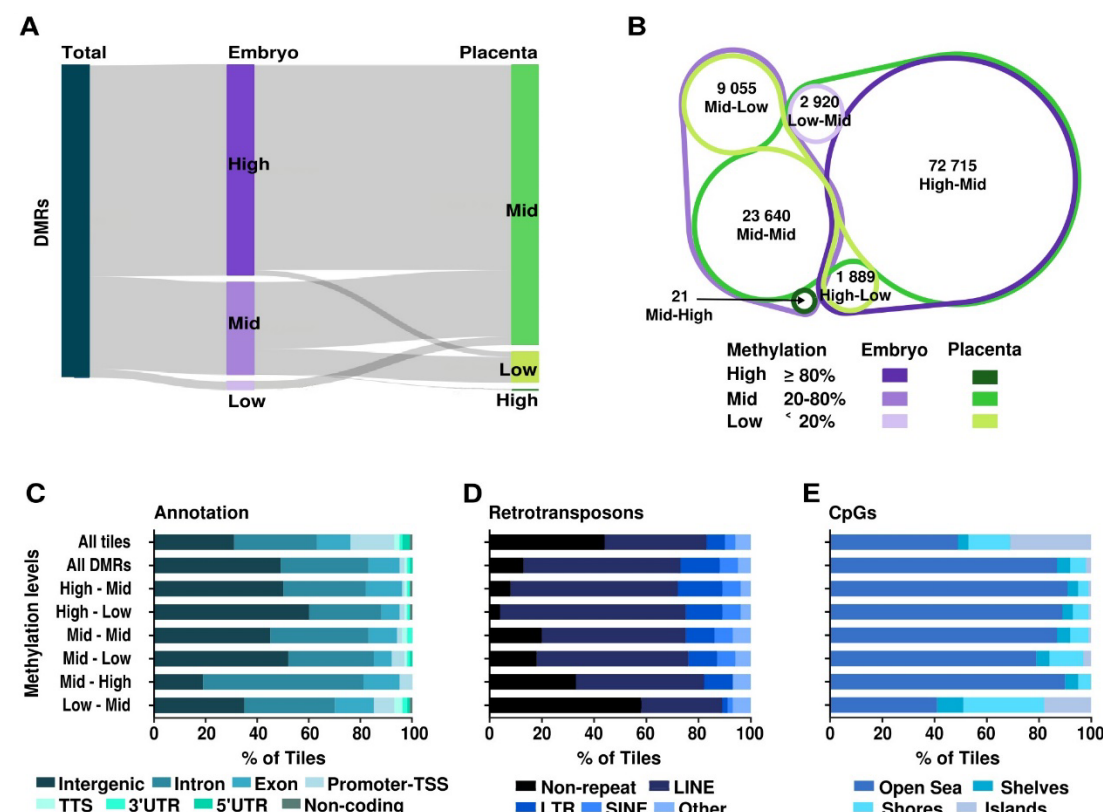761 methylation profiles (*Mir219a-2/Mir219b,* and *Sox6*) in placenta.
762

763
764
765 **Figure 3. Distinct genomic features in DMRs based on their methylation status in embryo**
766 **and placenta.** DMR analysis by methylation levels in embryo and placenta. **A)** Sankey diagram
767 dividing DMRs by methylation levels in embryo (*purple*) and placenta (*green*) for the associated
768 tiles. High : ≥80% methylation, Mid (intermediate) : ≥20% - <80% methylation , Low : <20%
769 methylation. **B)** Venn diagram showing the proportion of tiles in the different DMR categories
770 based on DNA methylation levels between embryo and placenta. **C), D)** and **E)** Analysis of all
771 tiles, all the DMRs, as well as the 6 different DMR categories based on levels of DNA
772 methylation in embryo and placenta for : **C)** Genomic annotations, **D)** Main retrotransposons and
773 **E)** Proximity of CpG rich regions. Neighboring CpG dense regions were defined as shore; up to
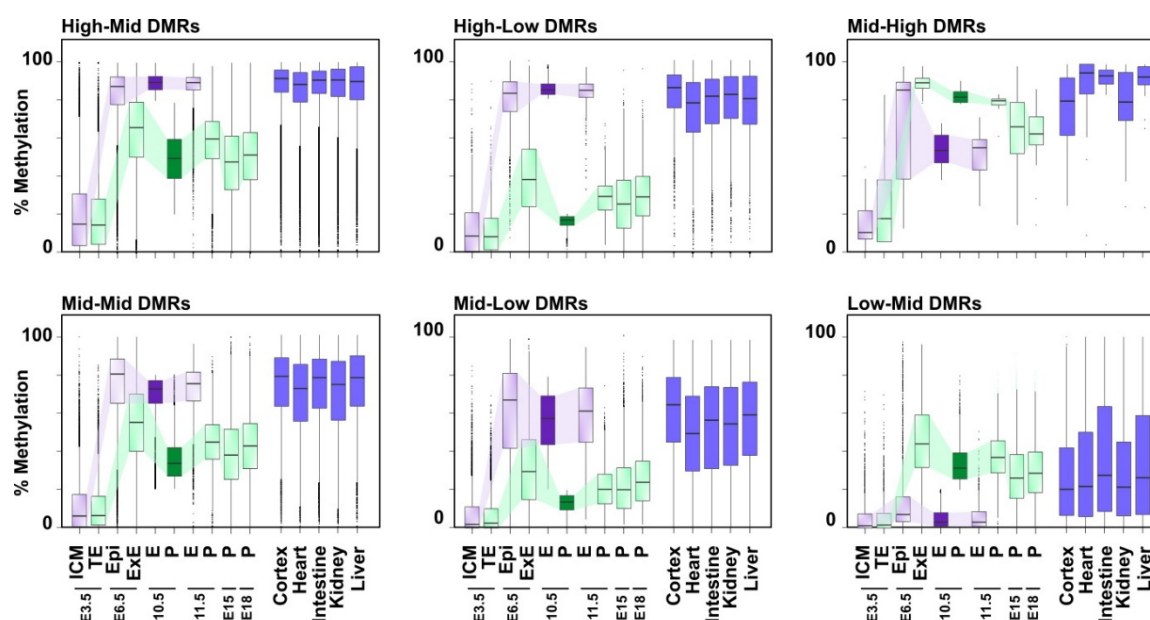774 2kb away from CGIs, shelf; 2-4kb away from CGIs, and open sea; >4kb away from CGIs.
775
776
777
778
779

780
781

782
783
784 **Figure 4. Dynamics of DNA methylation profiles associated with DMR categories and their**
785 **evolution across embryo and placenta development.** Box plots representing the DNA
786 methylation distribution and median values for each DMR category in various developmental
787 stages. Tiles associated with DMR categories at E10.5 were overlapped with previously
788 published and publicly available data, and methylation levels were determined at each
789 developmental stage (Smith et *al* 2012, Smith et *al*. 2014, Whidden et *al*. 2016) or in adult
790 somatic tissues (Hon et *al*. 2013). ICM: inner cell mass, TE: trophectoderm, Epi: epiblast, ExE:
791 extraembryonic ectoderm, E: embryo, Pla: placenta. See Table S2 for median and mean
792 methylation values, and Table S4 for number of overlapping tiles analysed.
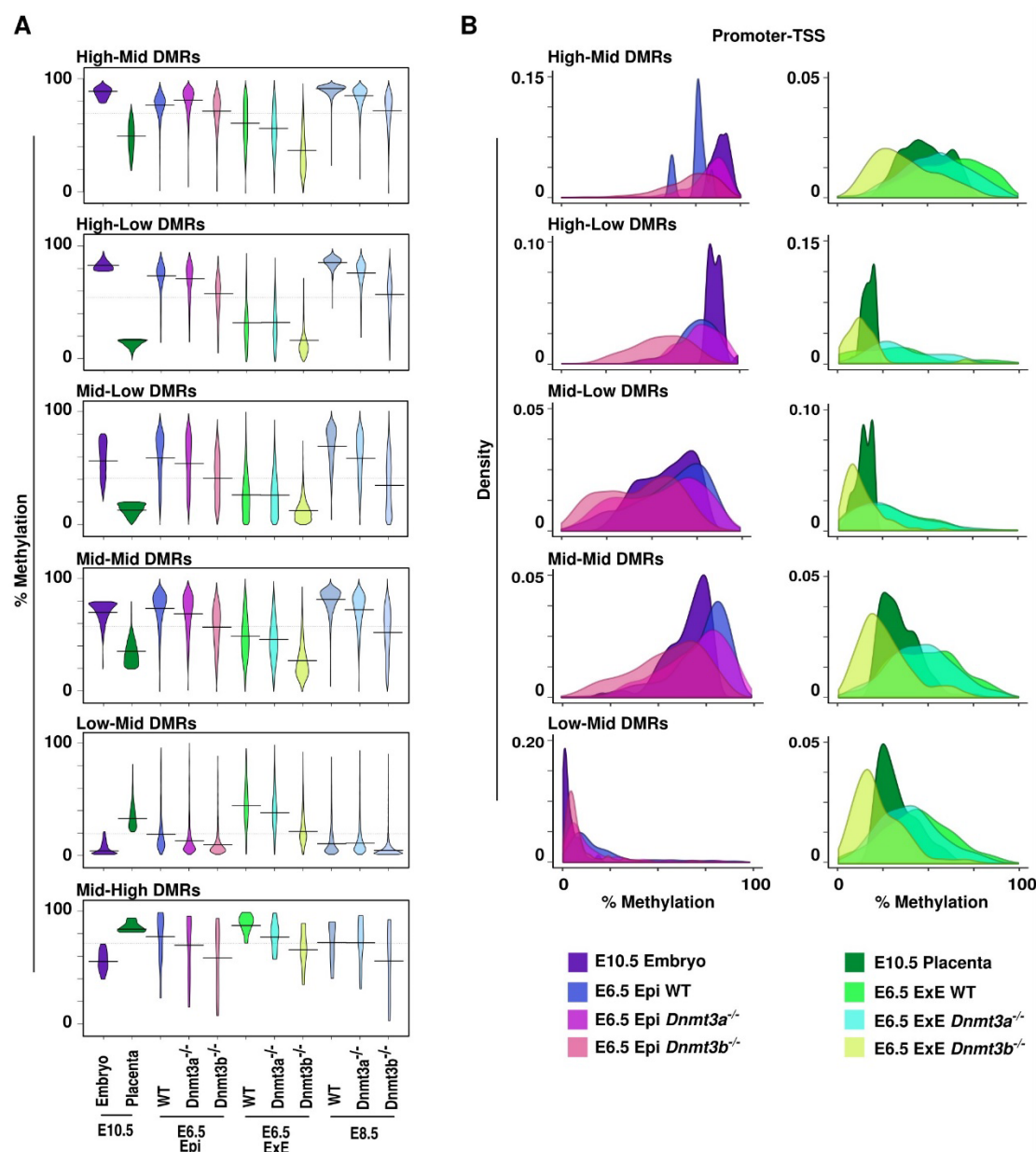
793
794
795
796
797
798
799
800
801
802
803

804
805
Figure 5. *Dnmt3a*- or *Dnmt3b*-deficiency alter proper establishment of DMR-associated patterns. A) Violin plot representing DNA methylation distribution and median values of tiles associated with the different DMR categories at E10.5, and their methylation levels in the different tissues and genotypes at E6.5 and E8.5. **B)** Promoter-TSS density graphs for E10.5 embryo and E6.5 epiblast (wt, *Dnmt3a$^{-/-}$* and *Dnmt3b$^{-/-}$*) (left panel) and for E10.5 placenta and E6.5 extraembryonic ectoderm (wt, *Dnmt3a$^{-/-}$* and *Dnmt3b$^{-/-}$*) (right panel). E: embryo, Epi: epiblast, ExE: extraembryonic ectoderm. See Table S3 for median and mean methylation values, and Table S4 for number of overlapping tiles analysed.
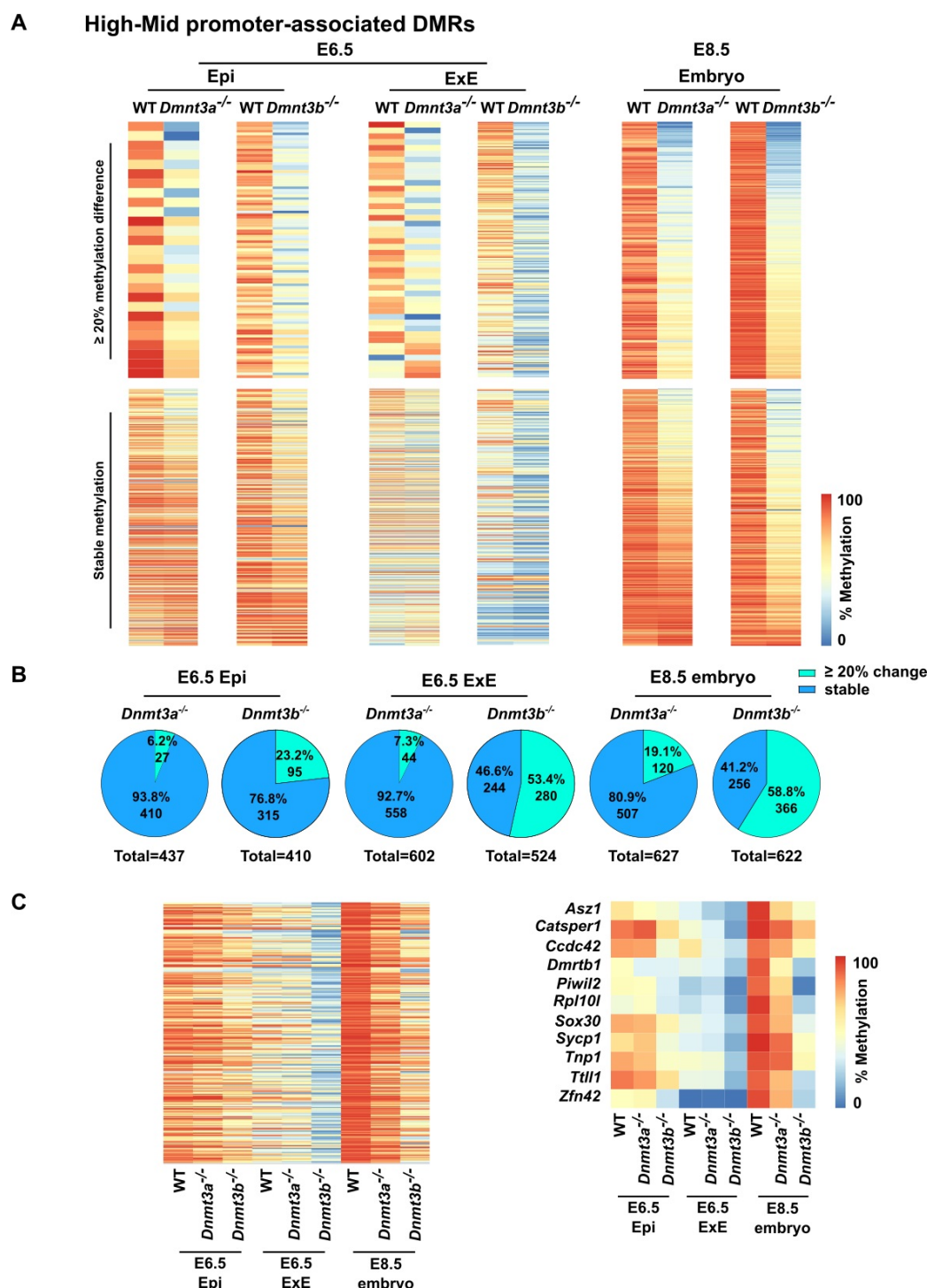
814
815

27

A High-Mid promoter-associated DMRs

Figure 6. Developmental decline in compensatory DNA methylation mechanism in response to *Dnmt3a*- or *Dnmt3b*-deficiency at promoter-TSS associated with High-Mid DMRs. A) Heatmaps comparing the DNA methylation profiles of wt vs *Dnmt3a⁻/⁻* or wt vs *Dnmt3b⁻/⁻* for E6.5 epiblast, E6.5 extraembryonic ectoderm or E8.5 embryo in 100bp tiles overlapping promoter-associated DMRs that are highly methylated in the embryo (≥80%) and mildly methylated in the placenta (≥20 and <80%). Upper panel represents regions with a difference of methylation of at least 20% between wt and *Dnmt3a⁻/⁻* or wt and *Dnmt3b⁻/⁻*. Lower panel

824   represents stable regions (lower than 20% difference in methylation). **B)** Pie charts representing
825   DMR numbers for each comparison. **C)** Heatmap of the methylation levels of tiles commonly
826   represented in all 9 public data samples that overlap with promoters-associated High-Mid DMRs
827   (n = 314 tiles) (left panel). Heatmap of the methylation level of gene associated with piRNA,
828   gamete generation and germ cells or meiotic nuclear division that are covered in all 9 public
829   datasets (right panel).
830